Estimation of Rain Intensity Spectra over the Continental US Using Ground Radar-Gauge Measurements

Xin Lin* and Arthur Y. Hou

Mesoscale Atmospheric Process Branch

NASA Goddard Space Flight Center, Code 613.1,

Greenbelt, MD 20771, USA

Submitted to *the Journal of Climate*

Corresponding author address:

Dr. Xin Lin,
Mesoscale Atmospheric Process Branch,
NASA Goddard Space Flight Center, Code 613.1,
Greenbelt, MD 20771.

Tel: 301-614-6146
E-mail: xlin.lin-1@nasa.gov

* Additional Affiliation: GESTAR/Morgan State University, Baltimore, MD 21251.

Abstract

A high-resolution surface rainfall product is used to estimate rain characteristics over the continental US as a function of rain intensity. By defining each data at 4-km horizontal resolutions and 1-h temporal resolutions as an individual precipitating/non-precipitating sample, statistics of rain occurrence and rain volume including their geographical and seasonal variations are documented. Quantitative estimations are also conducted to evaluate the impact of missing light rain events due to satellite sensors' detection capabilities.

It is found that statistics of rain characteristics have large seasonal and geographical variations across the continental US. Although heavy rain events (> 10 mm/hr.) only occupy 2.6% of total rain occurrence, they may contribute to 27% of total rain volume. Light rain events (< 1.0 mm/hr.), occurring much more frequently (65%) than heavy rain events, can also make important contributions (15%) to the total rain volume.

For minimum detectable rain rates setting at 0.5 and 0.2 mm/hr which are close to sensitivities of the current and future space-borne precipitation radars, there are about 43% and 11% of total rain occurrence below these thresholds, and they respectively represent 7% and 0.8% of total rain volume. For passive microwave sensors with their rain pixel sizes ranging from 14 to 16 km and the minimum detectable rain rates around 1 mm/hr., the missed light rain events may account for 70% of train occurrence and 16% of rain volume.

Statistics of rain characteristics are also examined on domains with different temporal and spatial resolutions. Current issues in estimates of rain characteristics from satellite measurements and model outputs are discussed.

1. Introduction

Statistics of rain intensity and frequency of occurrence have received more and more attention in recent years since the important climate trend affecting the hydrologic cycle and energy budget could be more clearly detected in the characteristics of rain events relative to the temporally- and spatially-averaged total rain accumulation (e.g., Englehart and Douglas 1985, Chen et al. 1996, Karl and Knight 1998, Meehl et al. 2000, Dai 2001, Trenberth et al. 2003, Groisman et al. 2005, Sun et al. 2006, Lau and Wu 2006, Dai et al. 2007). Figure 1 is a schematic showing the frequency distribution of rain events as a function of rain intensity between the climatology and an individual year. The areas covered below two colored curves represent the mean rain amount for the climatology and the individual year, respectively. Averaged over the globe or large domains, while the changes in the mean rain amount could be small and/or difficult to distinguish, the changes in the frequency distribution can be identified easily. Therefore, although the public attentions have been focusing mostly on changes in mean rain amount and limited numbers of devastating rain-producing weather events and severe droughts, it is ultimately the change/shift within the entire intensity spectrum of global or regional rain events that contribute to the short- and long-term climate variations in the hydrologic cycle.

Many observational studies have examined the characteristics of rain events in terms of rain intensity and frequency of occurrence (e.g., Englehart and Douglas 1985, Petty 1995, 1997, Karl and Knight 1998, Dai 2001, Trenberth et al. 2003, Short, 2003, Groisman et al. 2005, Lau and Wu 2006, Dai et al. 2007, Ebert et al. 2007, Berg et al. 2010). For example, Petty (1995) investigated frequencies and characteristics of global

oceanic precipitation from shipboard weather reports and noted large seasonal and geographic variations for different rain groups including thunderstorms and drizzles. Similarly, Dai (2001), using 3-hourly global weather reports, estimated the seasonal and inter-annual climatology of rain frequency over both land and ocean for various types of precipitation including drizzle and non-drizzle precipitation, showery and non-showery precipitation, thunderstorms, and snow. With quantitative information on precipitation rates, various thresholds of rain intensity or frequency of rain occurrence have been developed to categorize long-term observational rain data records and explore the climate trend affecting different rain event ensembles (e.g., Karl and Knight 1998, Groisman et al. 2005, Lau and Wu 2006). For example, Karl and Knight (1998), using long-term daily rain gauge data over the contiguous United States, found almost a 10% increase in the heavy and extreme daily precipitation events over the past century. Lau and Wu (2006) examined the probability distribution function of pentad tropical rainfall and noticed that two commonly-used satellite-ground-blended rain products all indicated a positive trend in the occurrence of heavy and light rain events during 1979-2003 and a negative trend in moderate rain events. More recently, Berg et al. (2010) collocated instantaneous satellite rainfall retrievals from a precipitation radar (PR) and a cloud profiling radar (CPR), and examined the entire rainfall intensity spectra over tropical and subtropical oceans. In addition to the advance in observational studies on rain characteristics, evaluations of model results using observational data based on statistics of rain intensity and frequency of rain occurrence have also provided key metrics for testing the influence of model physical parameterizations on the hydrological cycle (e.g., Chen et al. 1996, Meehl et al. 2000, Dai 1999, Trenberth et al. 2003, Sun et al. 2006, Dai. 2006, Ebert et al. 2007, etc).

Rain intensity and frequency of occurrence are strong functions of the temporal and spatial scales. Due to limited availability and quality of long-term station data records, many earlier observational studies on characteristics of rain events were based on rain rates averaged over a day or even longer, thus essentially provided estimations biased toward statistics of large rain systems with heavy and intermediate rainfall. Although light rain events are well known to occur much more frequently than heavy and intermediate rain events, there are large uncertainties in estimating contributions of light precipitation to rain incidence and rain volume (e.g., Petty 1995). For example, there could be two different types of "light rain" at daily time scale. It is possible that a region characterized by persistent, light precipitation throughout the day has the same daily mean rain rate as a region with intermittent, but heavy convective precipitation. Their impact on the vertical heating and moistening profiles as well as the surface water runoff and soil moisture can be drastically different. Using pointed station data to estimate averages over larger domains may induce large representativeness errors since precipitation is highly variable in the horizontal. Furthermore, applying the same rain intensity or rain frequency thresholds (say, 10 mm/day to distinguish heavy rain events) on domains of different horizontal resolutions (e.g., a 1ºx1º grid, vs. a 2.5ºx2.5º grid) could include many different rain event ensembles, thus potentially leading to contradicting statistics of rain characteristics. Given these concerns and uncertainties, it is important and necessary to quantitatively examine the characteristics of entire rain event spectra at fine temporal and spatial scales.

Satellite observations are widely utilized to extract instantaneous estimates of rainfall information on the global scale, providing a promising way to examine

characteristics of rain spectrum at fine temporal and spatial resolutions. Among various remote-sensing instruments, microwave sensors that directly respond to the absorption and scattering of cloud hydrometer particles provide the backbone of space-based precipitation measurements. However, the quality of rain retrievals varies with the sensitivity of satellite instruments and retrieval algorithms as well as sensor spatial resolutions. Each satellite rainfall retrievals has its own minimum detectable rain rate, in which below the threshold, its detection capability is quickly degraded (e.g., Petty 1995, 1997, Lin and Hou 2008, Berg et al. 2010). For example, the rain retrieval from the precipitation radar (PR: Meneghini and Kozu 1990; Kummerow et al. 1998, 2001; Iguchi et al. 2000) on board the Tropical Rainfall Measuring Mission (TRMM, Simpson et al. 1988, 1996) satellite has the minimum detectable rain rate ranging between 0.5 and 0.7 mm/hr at the footprint resolution of 5 km. Rain retrievals from passive microwave (PMW) sounders such as the Advanced Microwave Sounding Unit-B (AMSU-B) instruments on NOAA-15, -16, and -17 satellites have the minimum detectable rain rate of 1.1 mm/hr over land at the footprint resolution of 16 km (Dr. R. Ferraro from NOAA, personal communication). Rain retrievals from PMW imagers are more accurate than those from PMW sounder data over the ocean, but they tend to have similar uncertainties and similar minimum detectable rain rates over land as those from the sounder data. It is not clear how the varying detection capability could affect the contribution of different rain intensity categories to the total rain incidence and rain volume, and how the statistics of rain characteristics would change with rain samples averaged over different horizontal resolutions.

In this study, we use a high-resolution rainfall product derived from 8-year surface radar and gauge data to explore rain intensity spectra over the US continent. Statistics of rain occurrence and rain volume including their geographical and seasonal variations are documented between 2002 and 2009. In particular, we intend to estimate the fraction of light rain occurrence and volume, and try to assess the impact of a number of satellite sensors' detection capabilities due to missing light rain events. The precipitation product is at 4-km horizontal resolutions and at 1-h intervals covering the entire US continent, providing an excellent opportunity to estimate the complete rain intensity spectra over land at fine temporal and spatial resolutions and mimic what different satellite rain observations would detect.

The Global Precipitation Measurement (GPM) mission (Hou et al. 2011), being developed as an international science partnership, is planning to advance observations of precipitation to both the Tropics and higher latitudes with enhanced sampling frequencies and improved measuring capabilities. Specifically, GPM will have a Core satellite carrying a Dual-frequency Precipitation Radar (DPR) and a high-resolution, multi-channel PMW rain radiometer known as the GPM Microwave Imager (GMI), which has innovative capabilities to measure light rain and falling snow. Along with Core are a number of constellation satellites (with variable life cycles and different sensor characteristics) in sun-synchronous and non-sun-synchronous orbits, with each member having its unique scientific or operational objectives but contributing data to GPM to produce uniformly calibrated global precipitation products. The work reported in this paper involving rain detection capabilities of the current and future sensors will potentially provide important guidance to the GPM mission.

The purpose of the study is to 1) document the climatology of rain intensity spectrum distribution over the US continent using surface radar and gauge data, including their seasonal and regional variations; 2) examine the fraction of light rain occurrence and volume relative to the total rain occurrence and volume, thus providing preliminary estimates of rain events missed by satellite sensors due to their detection capabilities; 3) discuss and clarify some current issues in estimates of rain frequency and rain intensity from satellite measurements and model outputs. Section 2 introduces the dataset and analysis methodologies, and discusses sensitivity tests conducted to evaluate the contribution of heavy and light rain events. Section 3 presents the seasonal and regional climatology of rain characteristics over the US continent. Section 4 examines statistics of rain occurrence and rain volume, and investigates the impact of satellite sensors' detection capability on precipitation statistics. Sections 5 and 6 estimate sensitivities of rain characteristics on rainfall averaged on different temporal and spatial resolutions. Section 7 presents the final conclusions of the study.

2. Data and Analysis Methods

The surface rainfall data used in this study are the merged surface radar and rain gauge product from the National Centers for Environmental Prediction (NCEP) National Hourly Multi-Sensor Precipitation Analysis Stage IV (Lin and Mitchell 2005). The ground radar bias correction technique and the radar-gauge merging methodology are developed by Smith and Krajewski (1991) and Seo (1998), respectively. This data set collects hourly radar rainfall estimates from about 140 WSR-88D operational radars over the US continent, merging with about 3000 hourly gauge reports. The Stage IV data are

preliminarily quality controlled and calibrated. The precipitation product is on a 1121x881 polar stereographic grid, and is at the 4-km resolutions. It covers the entire US continent at 1-h intervals from 2002 to the present. Although it is understandable that there might still be some uncertainties on issues such as data quality and calibration, this merged surface rainfall dataset offers excellent "truth" information at fine temporal and spatial resolutions, with continuous sampling of various rain events over the continental US.

In the following sections (unless specifically mentioned), statistics of rain volume and rain occurrence are calculated as functions of rain intensity using the rain data at the 4-km resolutions and 1-h intervals as individual precipitating/non-precipitating samples. Horizontal distributions of mean rain amount and frequency of occurrence are also calculated in a similar way, but are tabulated onto a 1ºx1º grid.

One of the major objectives in this study is to estimate rain intensity spectra over land, and evaluate the impact of missing light rain events due to satellite sensor detection capability. Among the current and near-future active microwave sensors that provide rainfall measurements, the footprint resolution of the current TRMM PR rain pixel is about 5 km at nadir, and its minimum detectable rain rate is about 0.5 mm/hr. The DPR onboard the on-planning GPM mission CORE satellite will also have a footprint resolution of 5 km (for Ku-band), and the expected accuracy is 0.2 mm/hr sensitivities. It should be noted that these minimum detectable rain rates from PR and DPR are reasonable approximations and they could vary a little depending on the drop size distribution and the horizontal variability within the field of view (FOV). Nevertheless, the horizontal resolution of the merged surface rainfall product is close to the rain pixel

resolutions of both PR and DPR. As for temporal resolutions, the satellite rainfall retrievals from PR and DPR are snapshots for a period of less than a second while the surface radar and gauge merged rain product is an hourly dataset. Although the rain statistics from instantaneous measurements may be slightly different from the statistics from hourly averages, we assume that the characteristics of rain events do not change much within one hour, so that the hourly surface rainfall product is adequate to infer statistics of instantaneous satellite rainfall estimates. It should be pointed out that this steady-state assumption likely performs poorly in regions and seasons where transient showers dominate. This issue will be further discussed in sensitivity tests carried out in later sections. In order to compensate for some of the uncertainties arising from the difference in temporal and spatial resolutions between rain retrievals from space-borne radars and the surface rain product, four rain intensity thresholds: 0.2, 0.3, 0.5, 1.0 mm/h are used to estimate the impact of missing light rain events, with thresholds 0.2 mm/h and 0.5 mm/h more closely representing GPM DPR and TRMM PR's detection capability. Another rain intensity threshold, 10 mm/hr, is used to distinguish heavy rain events.

For many current PMW radiometers and sounders such as the TRMM Microwave Imager (TMI), the Special Sensor Microwave Imager (SSMI) on the Defense Meteorological Satellite Program (DMSP) F-13, -14 and -15 satellites, and the Advanced Microwave Scanning Radiometer for the Earth Observing System (AMSR-E) on the Aqua satellite, as well as the AMSU-B on NOAA-15, -16 and -17 satellites, their rain pixel sizes are typically larger than 5 km, and may vary with the frequency channels being used. Their minimum detectable rain rates also vary with the algorithms being used

as well as the land surface background. Their sensitivities on horizontal resolutions will be discussed and examined in Section 5.

3. Seasonal mean distributions

Many studies have examined the climatology of rain characteristics over the continental US based on gauge data and weather reports (e.g., Englehart and Douglas, 1985, Chen et al. 1996, Dai 2001, Sun et al. 2006, Dai 2006, 2007). Using the merged radar and gauge data at fine spatial and temporal resolutions, we re-examine the seasonal-mean distributions of rain amount, frequency of rain occurrence and rain intensity in Figure 2. For each 1ºx1º grid box over the continental US, each surface rainfall data at its original resolution (4-km horizontal resolution, and 1-h intervals) is considered as an individual sampling pixel. Mean rain amount here, following the same way as used in earlier studies, is defined as the ratio of the total accumulation of precipitation to the total number of sampling pixels within a 1ºx1º grid box for any given seasons. Similarly, mean frequency of rain occurrence is calculated as the ratio of the number of raining pixels to the total number of sampling pixels which is essentially the fraction of raining area relative to the total area. Mean rain intensity is calculated as the ratio of the total amount of precipitation to the total number of raining pixels.

Similar to what is found in earlier studies, there are large regional and seasonal variations in the climatology of rain characteristics over the US. During the summer season (June-July-August, Fig. 2a), the North American Monsoon combined with moisture from Gulf of Mexico bring frequent thunderstorms to the southern and central parts of US. Tropical cyclones from the Atlantic Ocean also bring significant amount of

precipitation to the southern and eastern parts of the US. As a result, large precipitation amounts can usually be noticed over the southeast part of the US during summer, especially along the coastal area. It gradually decreases toward inland. A maximum in frequency of rain occurrence (6-10%) can be observed extending from the southern states northeastward all the way to Maine. The central part of US also has frequent rain events, with a maximum of 5-6% over Nebraska-Oklahoma-Kansas located parallel to the orientation of the Rocky Mountain. This area, as noted by Wallace (1975), tends to feature frequent nocturnal thunderstorms. The average rain intensity is about 3-4 mm/hr. in the Gulf Coast area, and decreases to 2-3 mm/hr in higher latitudes. Comparing to the central and eastern parts of US, the mean rain amount over the western US is generally very light. While the Rocky Mountain area indicates some topography-related rain events (with likely some underestimations of small and shallow systems that ground radars can't detect due to the topography blocking), the West Coast region is very quiet with few rain activities during summer.

During the winter season (December-January-February, Fig. 2b), precipitation amount over the southeastern part of the US is significantly reduced. The largest mean rain amount is less than 5 mm/day and is located between Louisiana, Mississippi, and Tennessee. Frequent rain occurrence (10-20%), however, can still be observed over the central and eastern US. These precipitating events are likely to be associated with wintertime frontal systems featuring more persistent, lighter precipitation arising from large scale ascending. Mean rain intensity also gradually decreases from the Gulf Coast region to higher latitudes, suggesting a consistent transition of precipitating events from a more convective environment to an environment characterized by large-scale

ascending/descending. On the other hand, being associated with a major wintertime storm track, frequency of rain occurrence over the western US significantly increases in the winter with the maximum ranging between 20 and 40%. Although the mean rain intensity is light (less than 2 mm/hr), the mean rain amount over the northwest US is quite large. These broad features generally agree with what is found in earlier studies based on gauge data and weather reports (e.g., Chen et al., 1996, Dai 2001, Sun et al. 2006).

4. Rain intensity spectra

4a. Fractions of rain occurrence and volume

For rainfall estimations, some interesting yet still intriguing questions to ask are: what are the contributions of rain events within different rain intensity ranges to the total rain incidence and total rain volume? For a given minimum detectable rain rate, what percentage of rain occurrence and rain volume might be missed by certain satellite instruments? Such kind of exploration can provide very useful information on the impact of satellite sensor detection capabilities which could eventually lead to a better understanding of the short-term and long-term climate variability of light rain. Figure 3 depicts the fraction of rain occurrence as a function of rain intensity using all the merged high-resolution surface rainfall data over the US continent between 2002 and 2009. Values in each rain intensity bin are normalized by the total number of raining samples. Although no information is provided for the minimum detectable rain rate for the surface rainfall product, the number of raining samples drops rapidly and becomes negligibly small for rain intensity at and below 0.1 mm/hr, probably suggesting that the minimum detectable rain rate for the merged radar and gauge rainfall product is about 0.1 mm/hr.

As expected, light precipitation generally dominates the rain intensity spectra in terms of the fraction of rain occurrence over the continental US, with 62.5% of raining samples having rain rate less than 1 mm/hr (Figure 3). These are consistent with earlier findings over both land and ocean (Petty 1995, 1997, Dai 2006, Haynes et al. 2009, Berg et al. 2010) that light rain events tend to occur more frequently than heavy and intermediate rain events. The fraction of intermediate rain events (1.0 mm/hr < R < 10 mm/hr.) is 34.9%, about half of the fraction of light rain events. On the other hand, heavy rain events, defined as raining samples with rain rate > 10 mm/hr., occur much less frequently than light and intermediate rain events (with only about 2.6% of total rain incidence). For rain intensities setting at 0.2, 0.3, and 0.5 mm/hr, there are 11.3%, 24.5%, and 43.1% of total raining cells below these thresholds respectively. If we assume that 0.2 and 0.5 mm/hr are close to the thresholds that GPM DPR and TRMM PR are able to detect, the light rain occurrence that GPM DPR can detect but TRMM PR can't accounts for more than 30% of total rain occurrence.

The fraction of rain volume (Figure 4) indicates that heavy and intermediate rain events dominate the total rain volume falling over the continental US. Although heavy rain events occur much less frequently than light and intermediate rain events, they contribute about 27%, more than a quarter of the total rain volume. Combining both heavy and intermediate rain events, they contribute 84.6% of total rain volume over the US continent. On the other hand, the contribution of light rain events (below 1 mm/hr) is also very important, and can reach 15.4% of total rain volume. For rain intensity thresholds setting at 0.2, 0.3, and 0.5 mm/hr, their contributions to the total rain volume over the US continent are about 0.8%, 2.6%, and 7.0%, respectively. If we assume that

DPR and PR's minimum detectable rain rates are 0.2 and 0.5 mm/hr, DPR may only miss about less than 1% of total rain volume on its scan over land, while TRMM PR could miss more than 6% of total rain volume.

Berg et al. (2010) assessed the distribution of rain volume as a function of rain rate by employing collocated CloudSat CPR estimates below 1 mm/hr, and TRMM PR estimates above 2 mm/hr at 5-km resolution. They estimated that the rain volume contribution of oceanic rain rates below 0.2, 0.3, and 0.5 mm/h are 2.5%, 4.7%, and 8.3% respectively, very close to what obtained from surface radar and gauge product over land.

4b. Seasonal and geographical variations

As noted in Figure 2, both rain occurrence and rain volume have large seasonal and geographical variations across the continental US. Therefore the contributions of light and heavy rain events may also vary accordingly. Figure 5 shows seasonal variations of monthly fractions of rain occurrence and rain volume for rain rates less than 0.2, 0.3, 0.5, and 1.0 mm/hour, and for rain rate larger than 10 mm/hour.

Fraction of heavy rain occurrence is generally small throughout the year over the US continent. It follows the seasonal solar cycle with a maximum (5%) during the summer, and a minimum (1.3%) during the winter. For rain events with intensity below 1.0 and 0.5 mm/hr., their rain occurrence shows moderate seasonal variations with maxima during winter and minima during summer. The average fractions of rain occurrence range from 70% and 45% during the winter to about 55% and 40% during the summer. These seasonal variations, as shown in Figure 2, indicate seasonal transitions from persistent, light, large-scale precipitation during the cold season to vigorous,

intermittent, convective precipitation during the warm season. For lighter rain events, the seasonal variations are considerably small, and the fractions of rain occurrence are about 10%, and 25% for rain intensities below 0.2 and 0.3 mm/hr.

Although heavy rain events occur much less frequently than intermediate and light rain events, they make important contributions to the total rain volume throughout the year. Heavy rain events have a strong seasonal variation in fraction of rain volume, with a minimum of 13% in February and a maximum of 36% in July. This is consistent with the seasonal transition over the US continent from a large-scale, more baroclinic environment during the cold season to a more barotropic environment during the warm season featuring frequent, vigorous convection. The fraction of rain volume does not change much with seasons for rain events with rain intensity below 0.3 mm/hr.. The average fractions of rain volume are about 1% and 4% for rain rates below 0.2, and 0.3 mm/hr. For larger rain thresholds, their seasonal variations become larger, with the light rain contribution ranging from 10% during the winter to 6% during summer for rain events below 0.5 mm/h, and from 23% during the winter to 10% during summer for rain events below 1.0 mm/hr. Therefore TRMM PR, with a detectable rain rate of 0.5 mm/hr., could miss about 6-10% of total rain volume, while GPM DPR, with a detectable rain rate of 0.2 mm/hr., can capture about 99% of total rain volume throughout the year. Considering that the contribution of rain events with rain intensity below 0.1 mm/h (the possible threshold for the surface rainfall product) is likely much more smaller, these results suggest that without considering the orbital sampling issue, the contribution of light rain events that may be missed in GPM DPR scans will be negligibly small over the continental US in terms of total rain volume. Again it needs to be pointed out that the

minimum detectable rain rates for PR and DPR are not fixed, and they could vary significantly depending on the drop size distribution and the horizontal inhomogeneity within the FOV.

Figure 6 shows the horizontal distributions of fractions of rain occurrence and rain volume averaged over 8 summers (JJA) and 8 winters (DJF) for rain intensity thresholds above 10 mm/hr., and below 0.2, 0.5, 1.0 mm/hr. Similar to what is shown in Figure 2 for mean rain amount, and mean frequency of rain occurrence, there are large seasonal and geographical variations for heavy and light rain events in terms of rain occurrence and volume. In general, although heavy rain events occupy a small fraction of total rain incidence, they tend to make important contributions to the total rain volume. Light rain events usually account for a large fraction of total rain incidence, but they only contribute to a small fraction of total rain volume. During summer, the fraction of heavy rain occurrence shows maxima over the southern, southeastern, and central parts of the US, with 5-10% of rain events with rain intensity above 10 mm/hr. The corresponding fraction of rain volume also indicates a similar pattern with the contribution of heavy rain events to the total rain volume ranging between 30% and 50%. The western part of US, except for a narrow region along the California coast, indicates few heavy rain events. During winter, occurrence of heavy rain events is significantly reduced and is only limited near the coastal regions of the southern US. Except for some spotty areas, the volume fraction of heavy rain is generally smaller over the continental US. For rain events with rain intensity below 1.0 mm/hr, the area-averaged fractions of rain occurrence during summertime are about 60-90% over the western US, 50-60% over the central and northern US, and 40-50% over the southern and southeastern US. The

corresponding rain volume contribution ranges between 20-50% over the western US, 10-20% over the central and northern US, and below 10% over the southern and southeastern US. During wintertime, except for the area near the southern part of US which shows 40-60% of rain incidence for rain intensity below 1.0 mm/hr, most parts of the US are dominated with rain events with rain intensity below 1.0 mm/hr., indicating the significant contribution from persistent, light precipitation arising from large scale ascending. The volume fraction increases with latitudes varying from 10-20% over the southern and southeastern US to 60-90% over the northern US.

For rain events with rain intensity below 0.5 mm/hr, these are the rain event ensembles that may not be detected by TRMM PR. We can infer that light rain events missed by TRMM PR may account for 60-80% of rain incidence over the western US and 30-40% over the central and eastern US during summer. However, they only account for about less than 30% of total rain volume over the western US and less than 10% of total rain volume over the central and eastern US. During winter, the fraction of occurrence and volume increase over the northern US. The light rain volume missed by PR may account for about 40-60% of total volume near the wintertime storm track.

For rain events with the rain intensity threshold setting at 0.2 mm/hr., these are the rain event ensembles that may not be detected by GPM DPR. Except for the arid area over Idaho, Nevada, Utah and Arizona showing 30-50% of rain incidence and 5-10% of total rain volume, most parts of the US indicate smaller contributions of rain incidence (below 10%) and rain volume (below 2%). Therefore, despite the fact that the minimum detectable rain rate for PR and DPR are not fixed and could vary significantly depending on the drop size distribution and the horizontal inhomogeneity within the FOV, GPM

DPR has the capability to detect most rain events that contribute meaningfully to the total rain volume over the continental US, particular for the frequent light precipitation resulted from both warm season convection and cold season large-scale ascending.

In order to further examine the geographical variation of the light rain contribution, we co-locate the monthly-mean fractions of light rain occurrence and light rain volume with monthly mean rain amount on each 1ºx1º grid box. Therefore, for any given monthly mean rain amounts which can be easily calculated from data, the contribution of monthly-averaged light rain occurrence and light rain volume can be quantitatively estimated over the continental US.

Figure 7 shows the probability distribution function of the fraction of rain occurrence and fraction of rain volume as functions of monthly mean rain amount on a 1ºx1º grid box. Regions with larger monthly mean rain rates typically feature smaller fractions of light rain occurrence and light rain volume. For regions with monthly mean rain amount at 10 mm/day, the ensemble-mean fraction of light rain occurrence is about 5%, 15%, 25%, and 45% for rain events with rain intensities below 0.2, 0.3, 0.5, and 1.0 mm/hr. The corresponding fractions of light rain volume are 0.3%, 1.1%, 4.1%, and 9.2%. For regions with monthly mean rain amount at 1.0 mm/day, the ensemble-mean fraction of light rain occurrence is about 15%, 30%, 50%, and 73% for rain events with rain intensities below 0.2, 0.3, 0.5, and 1.0 mm/hr. The corresponding fractions of light rain volume are about 3.1%, 7.2%, 19.2%, and 36.4%. Therefore, if TRMM PR, which has a minimum detectable rain rate at 0.5 mm/hr., is used to sample a region with the monthly mean rain rate at 1.0 mm/day, it is possible that about 50% of raining samples, and 20% of total rain volume may be missed by PR. If GPM DPR, which has a minimum

detectable rain rate at 0.2 mm/hr., is used to sample a region with the monthly mean rain rate at 1.0 mm/day, there are only about 15% of raining samples, and 4% of total rain volume missing. Certainly for regions characterized by very low monthly rain amounts, although the relative contribution of light rain (either missed or detected) is likely very high, its absolute contribution remains pretty small therefore may not affect much on the local hydrological applications.

5. Variations at different horizontal resolutions

Results shown in previous sections are for rain intensity spectra at 4-km horizontal resolutions which are close to rain pixel sizes of TRMM PR and GPM DPR. For many current rainfall retrievals derived from PMW radiometers and sounders, their rain pixel sizes typically range from 14 to 16 km or even larger, and each sensor may have different minimum detectable rain rates over land and ocean. Since statistics of rain characteristics are strong functions of horizontal resolutions, the larger the averaging grid box, the more likely the rain intensity spectra tend to shift to lower rain rates until reaching the domain-mean rain intensity.

In order to comprehensively examine the sensitivity of rain characteristics on horizontal resolutions, the merged surface radar and gauge data at the original 4-km horizontal resolution are averaged onto domains ranging from 4 km to 96 km at 4 km intervals. Figure 8 shows the variations of fractions of rain occurrence and rain volume at different horizontal resolutions for rain intensity thresholds larger than 10 mm/hr., and smaller than 0.2, 0.3., 0.5 and 1.0 mm/hr. It provides an estimation of detection capability for all the satellite rainfall retrievals over land. General speaking, as the horizontal

averaging domain increases, fractions of light rain occurrence and volume tend to increase for a given rain intensity threshold. This is not surprising since more zero-rain pixels are likely included and may effectively reduce the domain-averaged rain rate. For TRMM PR and GPM DPR (minimum detectable rain rates at 0.5 and 0.2 mm/hr., and both rain pixels at 5-km horizontal resolutions), missed light rain events account for about 45% and 11% of total rain occurrence, and 7% and 1% of total rain volume. Results on the 14-16 km horizontal resolution can be used to infer the rainfall characteristics for PMW radiometers and sounders. For example, rainfall retrievals derived from AMSU-B sounders on-board the NOAA-15, -16, and -17 satellites have minimum detectable rain rates at 1.1 mm/hr. at rain pixel resolution of 16 km (R. Ferraro 2006, personal communication). The missed light rain events by AMSU-B therefore may account for about 70% of total rain occurrence and 16% of total rain volume over land. Rain retrievals from PMW radiometer data (TRMM TMI, DMSP/SSMI, and AQUA AMSR-E) have similar minimum detectable rain rates and rain pixel resolutions over land (14-15 km), therefore, they tend to have similar statistics on light rain occurrence and volume. On the other hand, it should also be kept in mind that current PMW retrievals over land are mainly empirically derived from scattering-based algorithms. They are less capable of detecting precipitation from warm-topped clouds (Petty 1999, Joyce et al. 2004, Huffman et al. 2007)

Many studies have used satellite rainfall data to evaluate model output in terms of rain occurrence and rain intensity and to examine their variations associated with climate change. By doing so, satellite data are usually averaged onto model grid box sizes, and fixed rain intensities (1 mm/hr., or 10 mm/hr.) are used as thresholds to distinguish light

and heavy rain events respectively. However, the included rain event ensembles may be different for the same rain intensity threshold at different horizontal resolutions. Figure 8 further illustrates that fraction of heavy rain occurrence accounts for about 0.2%, 0.06% and 0.01% of total rain incidence at 25 km, 50 km, and 100 km resolutions for rain intensity larger than 10 mm/hr., and they may contribute to about 17%, 11% and 6% respectively of the total rain volume. On the other hand, if 1.0 mm/hr. is used as a cut-off rain rate to define light rain events, they can account for 76%, 83%, and 90% of total rain occurrence and contribute to about 18%, 24%, and 32% of total rain volume. Therefore caution should be taken when interpreting results of rain occurrence and rain volume averaged on different horizontal resolutions.

6. Sensitivities on temporal resolutions

Under the assumption that the characteristics of rain events do not change much within an hour, instantaneous satellite rainfall estimations are simulated using hourly surface radar and gauge data to examine the impacts of satellite sensors' detection capability on rain volume and rain occurrence as shown in the above sections. Precipitation, however, can be highly variable and is well known to be a strong function of temporal resolutions, particularly for those transient light rain events which could develop and dissipate within a very short time. In order to evaluate the steady-state assumption, a sensitivity test is conducted in this section using the on-going next generation Quantitative Precipitation Estimates (Q2) product (Vasiloff et al. 2007). This experimental Q2 rainfall product, being jointly developed by NOAA and university research communities, is on 1-km resolutions and provides rainfall estimations over the

entire US continent at 5-minute intervals. The primary sensor used in Q2 is the WSR-88D operational radar, with updated rain-reflectivity algorithms. A minimum detectable rain rate of 0.25 mm h^{-1}, corresponding to the lowest rain amount (0.01 inch) that a rain gauge could observe/record, is used in the original data to reduce contaminations of radar errors associated with ground clutter and non-precipitating targets (Dr. Pierre-Emmanuel Kirstetter from NOAA, personal communication).

One-month of original Q2 rainfall data (May 2010, courtesy of Professor Hong Yang, University of Oklahoma) are first horizontally averaged onto 4-km resolutions, and then temporally averaged to durations of 10, 20, 30, 40, and 60 minutes. Shown in Figure 9 are fractions of rain occurrence and rain volume as a function of temporal resolutions. Fractions of rain incidence for heavy rain ($R > 10$ mm h^{-1}) and intermediate rain (1 mm $h^{-1} < R < 10$ mm h^{-1}) events decrease slightly with longer averaging time intervals. The heavy and intermediate rain events are usually associated with large, more organized rain systems with life time typically longer than a few hours, and they are expected to have similar fractions of rain occurrence. For light rain events, fractions of rain occurrence tend to increase slightly as the averaging duration becomes longer since many zero-rain samples could effectively reduce the averaged rain rate. The lighter the rain events, the larger the fraction difference between data averaged over 5 minutes and data averaged over 60 minutes, indicating that the steady-state assumption indeed becomes weaker for highly transient cases such as fast-evolving convection and/or short-lived shower. These mesoscale and small-scale features could sometimes bring large biases to the regional and seasonal rain statistics, particularly during spring and summer when transient convection dominates. During the cold season when wide-spread and

persistent precipitation arising from large-scale ascending dominates, the sensitivity of rain incidence on temporal resolution is likely to be small. On the other hand, fractions of rain volume for light rain events indicate that their values do not change much with varying temporal resolutions. The heavy and intermediate rain events do indicate some sensitivity on temporal resolutions and these variations are probably associated with temporal and horizontal inhomogeneity so that some rain events fall to the intermediate rain category from the heavy rain category after averaging. Overall, although there are biases associated with transient precipitation events, it is generally a valid assumption to use hourly surface rainfall data to simulate instantaneous satellite rainfall estimations and examine the impacts of satellite sensors' detection capability on rain volume and rain occurrence.

7. Summary and discussions

Accurate estimations of rain intensity spectra provide an essential approach to evaluate the impact of climate trends on the hydrological cycle and energy budget. In this study, a high-resolution rainfall product merging surface radar and gauge data, the NCEP National Hourly Multi-Sensor Precipitation Analysis Stage IV (Lin and Mitchell 2005), is used to estimate rain characteristics over the continental United States as a function of rain intensity. By defining each data at 4-km horizontal resolutions and 1-h temporal resolutions as an individual precipitating/non-precipitating sample, the climatology of rain incidence and rain volume statistics including their geographical and seasonal variations is documented over an 8-year period between 2002 and 2009.

Consistent with many earlier studies on the climatology of rain characteristics (e.g., Chen et al. 1996; Dai 2001; Trenberth et al. 2003, Sun et al. 2006, Dai et al. 2007), mean rain amount, mean rain frequency, and mean rain intensity have large seasonal and geographical variations across the continental US. During the warm season, the central, southern, and eastern parts of the US, being influenced by the North America Monsoon and Atlantic hurricanes, receive large precipitation amount with frequent convective rain events. The West Coast region, mainly under the control of a strong subtropical high off the California coast, is generally very quiet with few rain activities. During the cold season, the central and eastern US still feature frequent rain occurrence but mean rain amount and rain intensity reduce significantly, reflecting a seasonal transition of rain events frequented by persistent, light precipitation arising from large scale ascending.

Averaged over the continental US, the high-resolution surface rainfall product indicates that heavy rain events (> 10 mm/hr.), although occupying only 2.6% of total rain occurrence, may contribute to 27% of total rain volume. Light rain events (< 1.0 mm/hr.), occurring much more frequently (65%) than heavy rain events, can also make important contributions (15%) to the total rain volume.

Quantitative estimations are also conducted to evaluate the impact of missing light rain events due to satellite sensors' detection capabilities. Results indicate that for minimum detectable rain rates setting at 0.5 and 0.2 mm/hr which are close to sensitivities of the current and near-future space-borne precipitation radars TRMM PR and GPM DPR, there are about 43.1% and 11.3% of total rain occurrence below these thresholds, and they respectively represent 7% and 0.8% of total rain volume. These statistics obtained from rainfall observations over land are close to those estimated over

the tropical and subtropical oceans (e.g., Berg et al. 2010). Further examination of fractions of rain occurrence and rain volume over different seasons and different geographical locations confirms that although the volume contribution of light rain events missed by the current TRMM PR could be still large, it will be negligibly small when the future GPM DPR is operational.

PMW radiometers and sounders are the backbone of space-based precipitation measurements. Their rain pixel sizes are considerably larger than 4-km resolutions and their minimum detectable rain rates may vary significantly, particularly over land. Statistics of rain occurrence and rain volume are further examined on different spatial domains for given rain intensity thresholds, providing a useful guide for many other satellite sensors' rain detection capabilities. For passive microwave sensors with their rain pixel sizes ranging from 14km to 16 km and the minimum detectable rain rate at 1 mm/hr., the missed light rain events may account for about 70% of total rain occurrence and 16% of total rain volume over land.

The estimation of precipitation characteristics is very sensitive not only to the temporal and spatial scales but also to the observational data quality and applicability. In this study, a number of potential biases in the data and analysis methodologies are noted and they could bring some uncertainties to the estimation of regional rain characteristics and evaluation of satellite sensors' detection capabilities. For example, (1) the merged surface rainfall product is likely to have significant biases in regions of snowfall due to the current surface radar's incapability to accurately retrieve wintertime solid precipitation; (2) instantaneous satellite observations are simulated using hourly surface data and such a steady-state assumption may be less valid when and where transient

and/or short-lived rain systems dominate; (3) the minimum detectable rain rate may vary with different hydrometeor profiles and the inhomogeneity within the FOV, as well as land surface backgrounds particular for PMW radiometers and sounders. It also needs to be pointed out that in addition to minimum detectable rain rates typically used in satellite observations, the fraction of precipitation could be missed due to maximum detectable rain rates resulted from the sensor signal saturation. No matter how perfect the retrieval algorithm is within the range that the sensor can measure, the truncation rain thresholds at the high and low ends can lead to significant biases in statistics of precipitation volumes and frequency of occurrence, and these biases may be also strong functions of the location and season as well as the time-space averaging. Therefore careful considerations must be taken when evaluating and interpreting satellite-observed and simulated climate trends in terms of frequencies of rain occurrence and rain volume.

Further studies are underway to explore rain characteristics changes that are associated with short-term climate variations. The seasonal-mean diurnal variation of rain intensity spectra will also be examined using the high-resolution surface rainfall data. These analyses could provide more objective information on the impact of satellite sampling and retrieval errors as well as the applicability of satellite-model comparisons in terms of the rain intensity spectra.

Acknowledgements

The NCEP surface radar and gauge Stage IV data are obtained from National Center for Atmospheric Research Earth Observing Laboratory. Thanks for Professor Hong Yang at University of Oklahoma for providing one-month Q2 rainfall data used for the sensitivity test. Special thanks for three anonymous reviewers for very constructive comments that greatly improve the paper. This research is supported by the GPM Project at the NASA Goddard Space Flight Center in Greenbelt, MD.

References

Berg, W., T. L'Ecuyer, and J. M. Haynes, 2009: The distribution of rainfall over oceans from spaceborne radars. Journal of Applied Meteorology and Climatology, 49, 535-543.

Chen, M., R. E. Dickinson, X. Zeng, and A. N. Hahmann, 1996: Comparison of precipitation observed over the continental United States to that simulated by a climate model. Journal of Climate, 9, 2233-2249.

Dai, A. G., 2001: Global precipitation and thunderstorm frequencies. Part I: Seasonal and interannual variations. Journal of Climate, 14, 1092-1111.

Dai, A. G., 2006: Precipitation characteristics in eighteen coupled climate models. Journal of Climate, 19, 4605-4630.

Dai, A. G., X. Lin, and K.-L. Hsu, 2007: The frequency, intensity, and diurnal cycle of precipitation in surface and satellite observations over low- and mid-latitudes. Clim. Dyn., 29, 727-744.

Ebert, E. E., J. E. Janowiak, and C. Kidd, 2007: Comparison of near-real-time precipitation estimates from satellite observations and numerical models. BAMS, 88, 47-64.

Englehart, P. J., and A. V. Douglas, 1985: A statistical analysis of precipitation frequency in the conterminous United States, including comparisons with precipitation totals. Journal of Climate and Applied Meteorology, 24, 350-362.

Groisman, P. Y., R. W. Knight, D. R. Easterling, T. R. Karl, G. C. Hegerl, and V. N. Razuvaev, 2005: Trends in intense precipitation in the climate record. J. Climate, 18, 1326-1350.

Haynes, J. M., T. S. L'Ecuyer, G. L. Stephens, S. D. Miller, C. Mitrescu, N. B. Wood, and S. Tanelli, 2009: Rainfall retrieval over the ocean with spaceborne W-band radar. J. Geophys. Res., 114, D00A22, doi:10.1029/2008JD009973.

Hou, A. Y., and Co-authors, 2011: The Global Precipitation Measurement (GPM) Mission. Conditionally accepted by *Bulletin of the American Meteorological Society*.

Huffman, G. J., R. F. Adler, D. T. Bolbin, G. Gu, E. J. Nelkin, K. P. Bowman, Y. Hong, E. F. Stocker, and D. B. Wolff, 2007: The TRMM multi-satellite precipitation analysis (TMPA): Quasi-global, multi-year, combined-sensor precipitation estimates at fine scales. J. of Hydrometeorology, 8, 38-55

Iguchi, T., T. Kozu, R. Meneghini, J. Awaka, K. Okamoto, 2000: Rain-profiling algorithm for the TRMM precipitation radar. Journal of Applied Meteorology, 39, 2038-2052.

Joyce, R. J., J. E. Janowiak, P. A. Arkin, and P. Xie, 2004: CMORPH: A method that produces global precipitation estimates from passive microwave and infrared data at high spatial and temporal resolution. J. Hydrometeor., 5, 487-503.

Karl, T. R., and R. W. Knight, 1998: Secular trends of precipitation amount, frequency, and intensity in the United States. Bull. Amer. Meteor. Soc., 79, 231-241.

Kummerow, C., W. Barnes, T. Kozu, J. Shiue, and J. Simpson, 1998: he Tropical Rainfall Measuring Mission (TRMM) sensor package. J. Atmos. Oceanic Technol., 15, 809-817.

Lau, K.-M., and H.-T. Wu, 2006: Detecting trends in tropical rainfall characteristics, 1979-2003. International Journal of Climatology, 27, 979-988.

Lin, X., and A. Y. Hou, 2008: Evaluation of coincident passive microwave rainfall estimates using TRMM PR and ground measurements as references. Journal of Applied Meteorology and Climatology, 47, 3170-3187.

Lin, Y., and K. E. Michell, 2005: The NCEP Stage II/IV hourly precipitation analyses: development and application. Preprints, 19th Conf. On Hydrology, American Meteorological Society, San Diego, CA, 9-13 January 2005, P. 1-2.

Meehl, G. A., F. Zwiers, J. Evans, T. Knutson, L. Mearns, and P. Whetton, 2000: Trends in extreme weather and climate events: Issues related to modeling extremes in projections of future climate change. Bull. Amer. Meteor. Soc., 81,427-436.

Meneghini, R., and T. Kozu, 1990: Spaceborne Weather Radar. Artech House, Boston, 197 pages.

Petty, G. W., 1995: Frequencies and characteristics of global oceanic precipitation from shipboard present-weather reports. Bull. Amer. Meteor. Soc., 76, 1593-1616.

Petty, G. W., 1997: An intercomparison of oceanic precipitation frequencies from 10 special sensor microwave/imager rain rate algorithms and shipboard present weather reports. J. Geophys. Res., 102, 1757-1777.

Petty, G. W., 1999: Prevalence of precipitation from warm-topped clouds over eastern Asia and the Western Pacific. *Journal of Climate*, 12, 220-229

Seo, D.-J., 1998: Real-time estimation of rainfall fields using rain gauge data under fractional coverage conditions. J. Hydrol., 208, 25-36.

Short, D. A., 2003: Equatorial Atlantic rain frequency: An intercentennial comparison. Journal of Climate, 16, 2296-2301.

Simpson, J., R. F. Adler, and G. R. North, 1988: A proposed Tropical Rainfall Measuring Mission (TRMM) satellite. *Bull. Amer. Meteor. Soc*., 69, 278-295.

Simpson, J., C. Kummerow, W.-K. Tao, and R. F. Adler, 1996: On the tropical Rainfall Measuring Mission (TRMM). *Meteor. Atmos. Phys*., 60, 19-36.

Smith, J. A., and W. F. Krajewski, 1991: Estimation of the mean field bias of radar rainfall estimates. J. Appl. Meteor., 30, 397-412.

Sun, Y., S. Solomon, A. Dai, and R. W. Portmann, 2006: How often does it rain? Journal of Climate, 19, 916-934.

Trenberth, K. E., A. Dai, R. M. Rasmussen, and D. B. Parsons, 2003: The changing character of precipitation. Bull. Amer. Meteor. Soc., 84, 1205-1217.

Vasiloff, S. V., and co-authors, 2005: Improving QPE and very short term QPF. Bull. Amer. Meteor. Soc., 86, 1899-1911.

Wallace, J. M., 1975: Diurnal variations in precipitation and thunderstorm frequency over the conterminous United States. Mon. Wea. Rev., 103, 406-419.

List of Figures

Figure 5: Seasonal variations of fraction of rain occurrence (the upper panel) and fraction of rain volume (the lower panel) for rain rates less that 0.2, 0.3, 0.5, and 1.0 mm/hour, and for rain rate larger than 10 mm/hour.

Figure 6a: Horizontal distributions of fraction of rain occurrence during the summer (JJA) and the winter (DJF) for rain intensity thresholds below 0.2, 0.5, 1.0 mm/hr., and above 10 mm/hr.

Figure 6b: Horizontal distributions of fraction of rain volume during the summer (JJA) and the winter (DJF) for rain intensity thresholds below 0.2, 0.5, 1.0 mm/hr., and above 10 mm/hr.

Figure 7: Fractions of rain occurrence (%) and rain volume (%) as functions of monthly mean rain rate derived on 1ºx1º grid.

Figure 8: Variations of fractions of rain occurrence and rain volume as a function of horizontal resolutions for rain intensity thresholds larger than 10 mm/hr., and smaller than 0.2, 0.3, 0.5, and 1.0 mm/hr.

Figure 9: Variations of fractions of rain occurrence and rain volume as a function of temporal resolutions for rain intensity thresholds larger than 10 mm/hr., and smaller than 0.2, 0.3, 0.5, and 1.0 mm/hr.

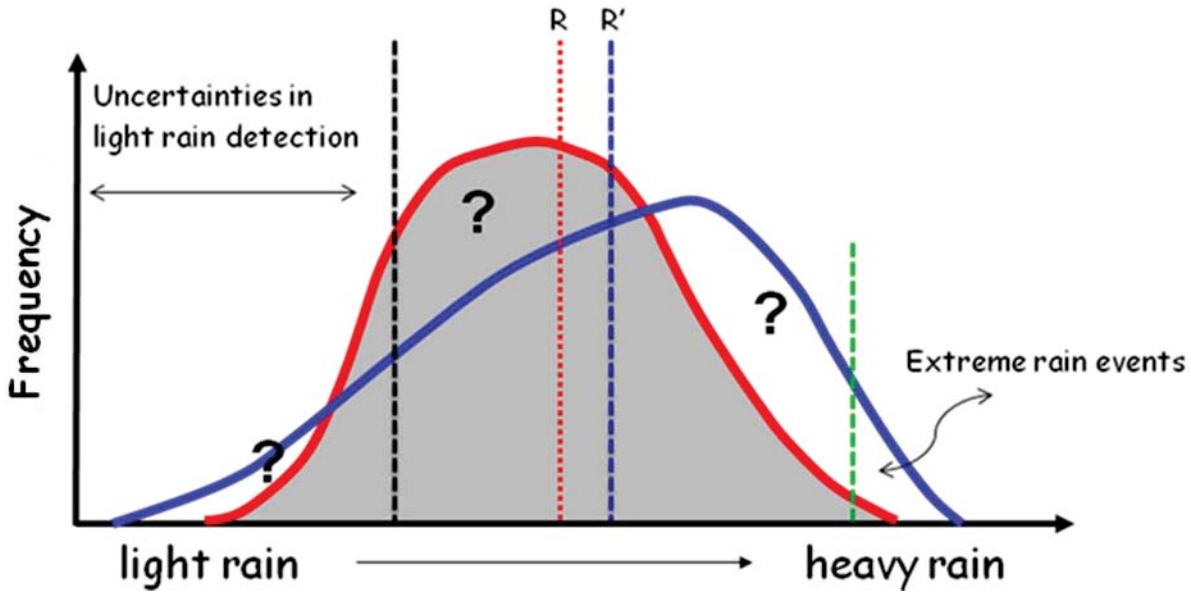

Figure 1: A schematic showing the total frequency of precipitation occurrence as a function of rain intensity for the climatology (red) and an individual year (blue). The areas covered below the red and blue curves represent their mean rain amount, and the two colored dashed lines in the vertical represent their mean rain intensities. The black dashed line in the vertical indicates the minimum detectable rain rate of individual observational instruments. The green dashed line in the vertical represents a threshold usually used to define extreme rain-producing events.

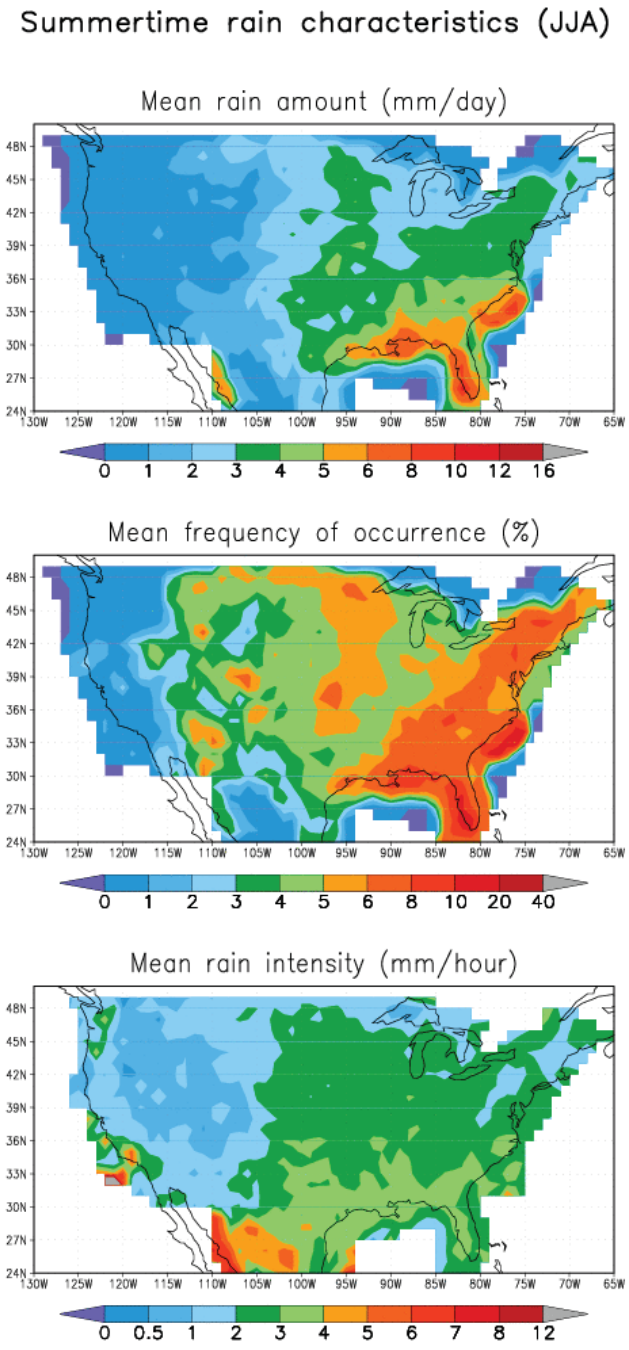

Figure 2a: Summertime mean distributions of rain amount (mm/day), frequency of occurrence (%), and rain intensity (mm/hour) over the US continent based on hourly radar and gauge data between 2002 and 2009.

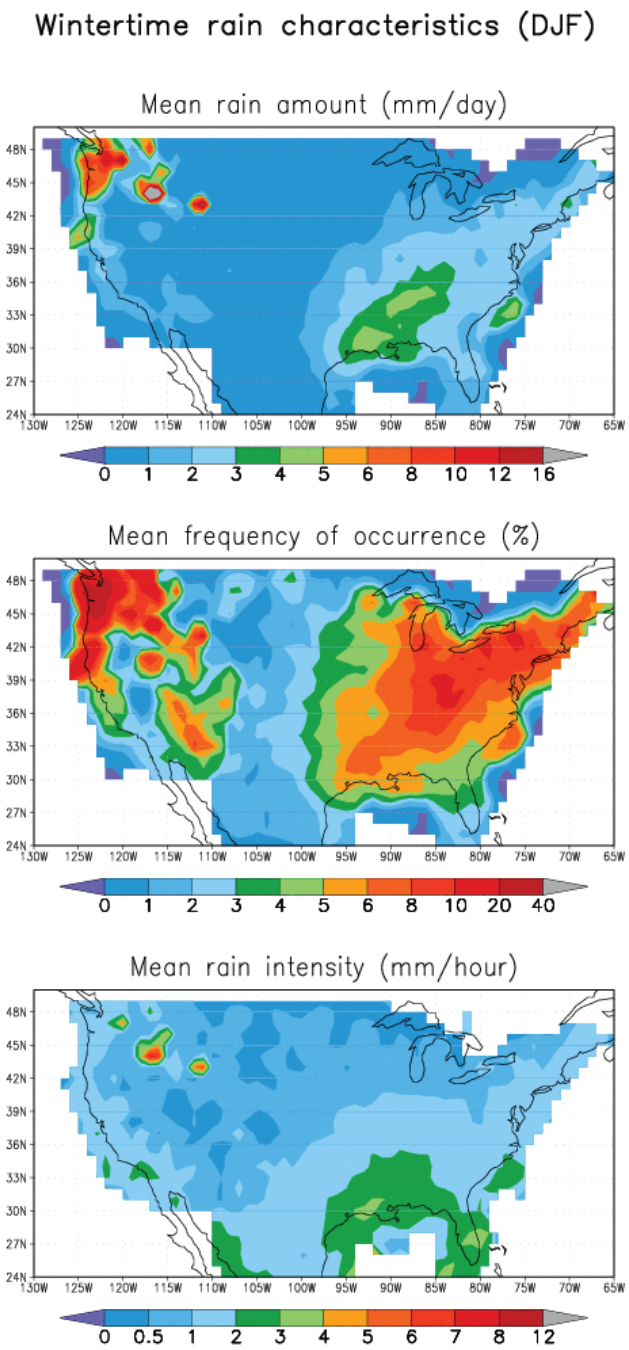

Figure 2b: Wintertime mean distributions of rain amount (mm/day), frequency of occurrence (%), and rain intensity (mm/hour) over the US continent based on hourly radar and gauge data between 2002 and 2009.

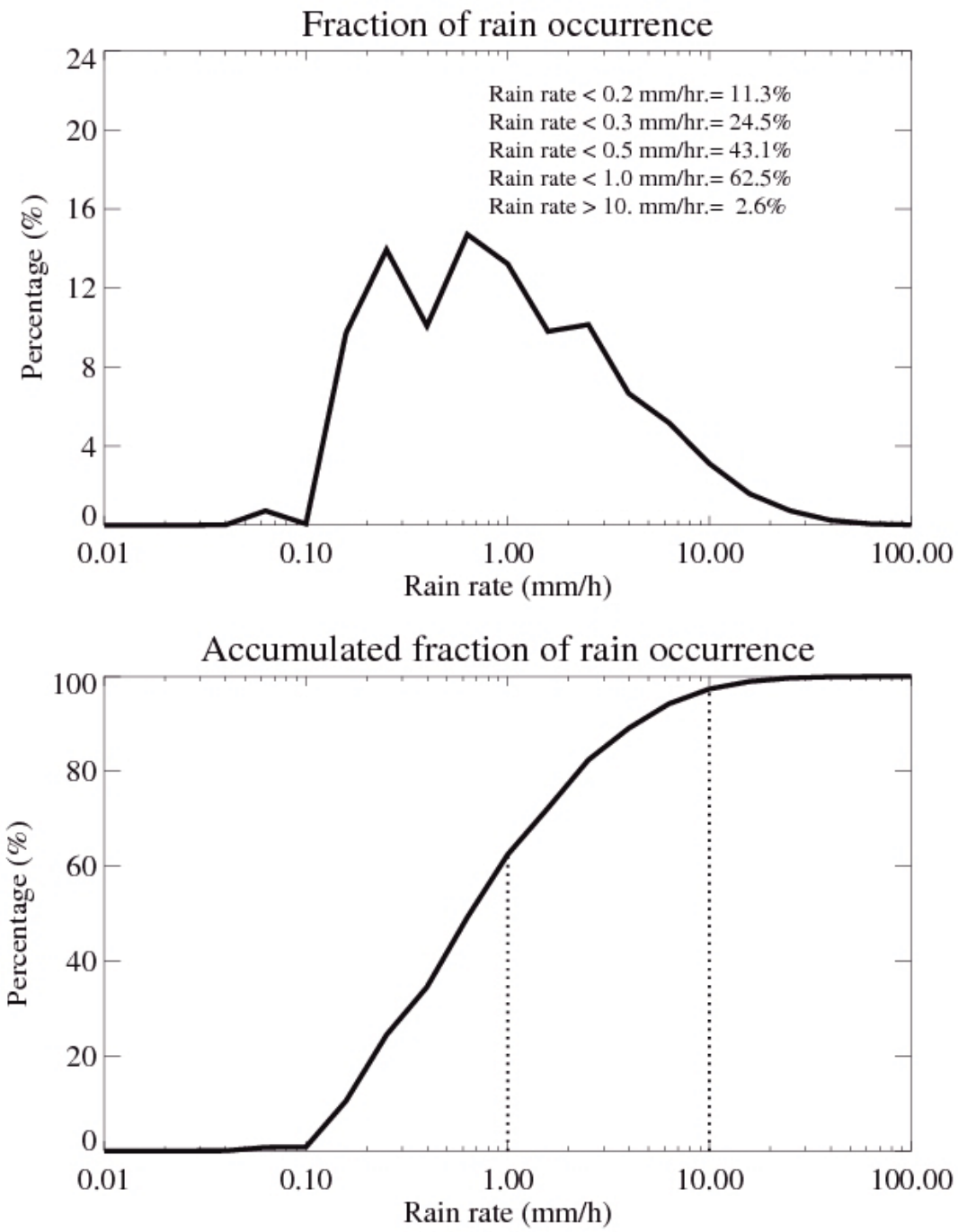

Figure 3: Fraction of rain occurrence (the upper panel) and accumulated fraction of rain occurrence (the lower panel) as functions of rain intensity for rain events between 2002 and 2009 over the US continent. Values in each rain intensity bin are normalized by the total number of raining samples.

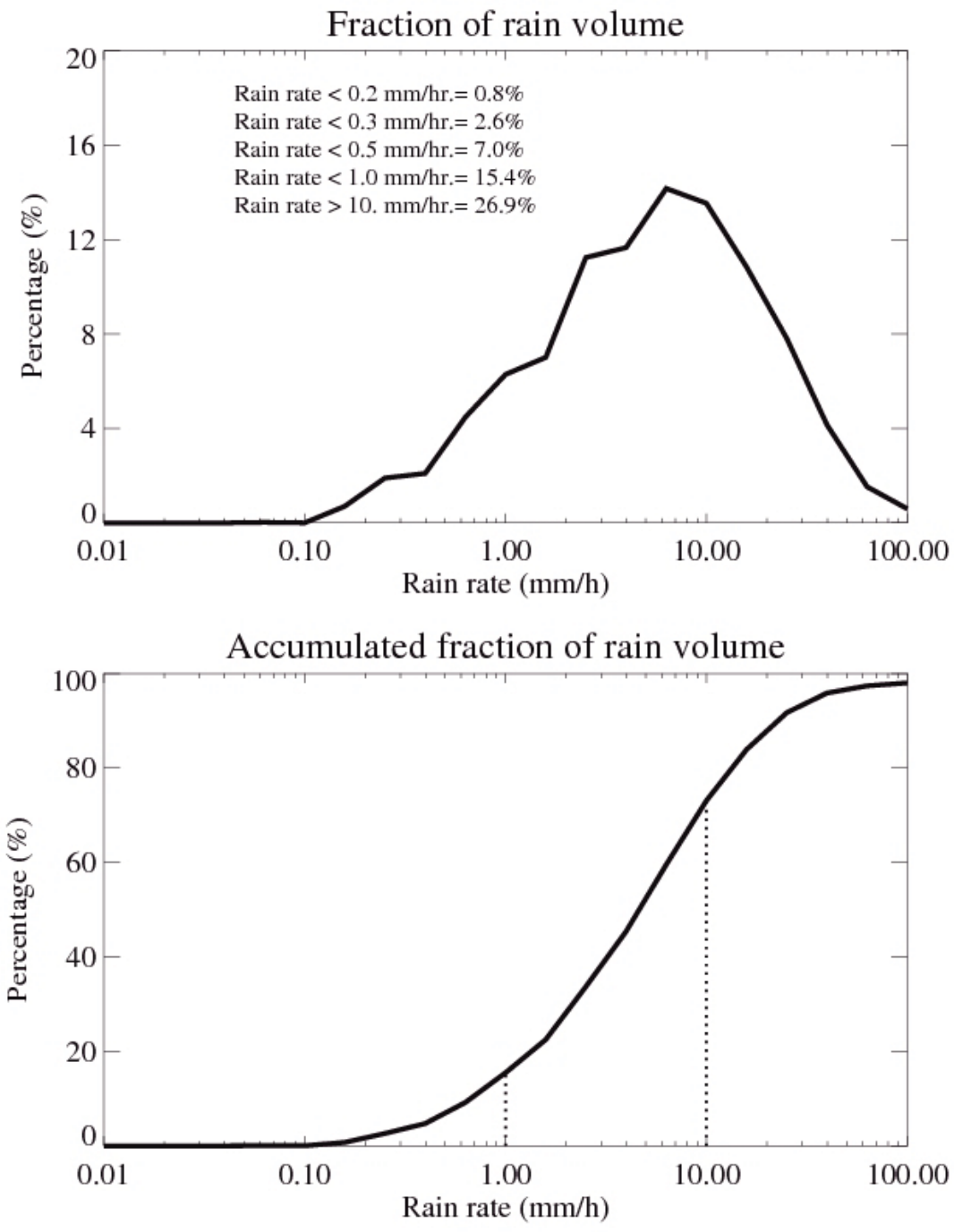

Figure 4: Fraction of rain volume (the upper panel) and accumulated fraction of rain volume (the lower panel) as functions of rain intensity for rain events between 2002 and 2009 over the US continent.

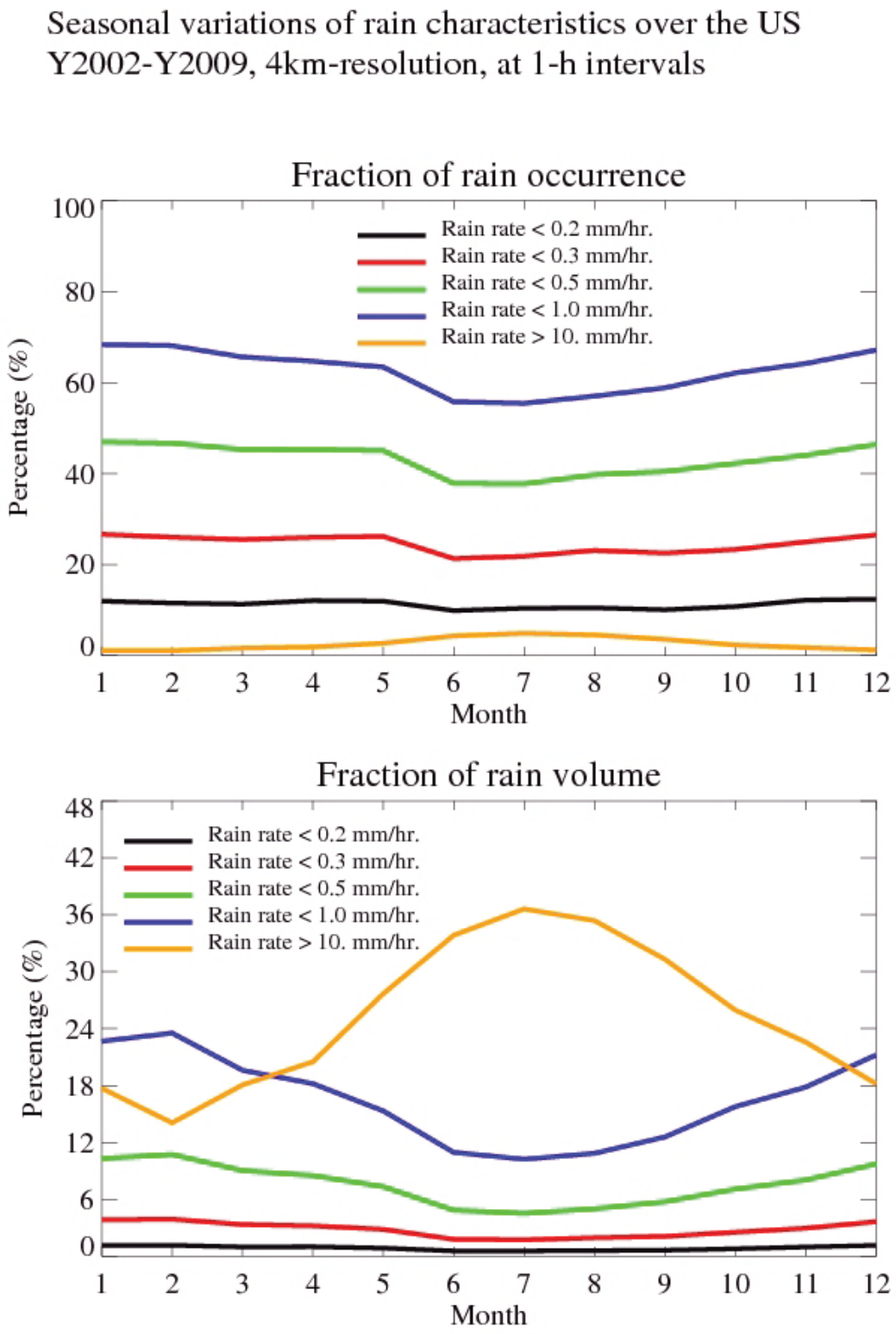

Figure 5: Seasonal variations of fraction of rain occurrence (the upper panel) and fraction of rain volume (the lower panel) for rain rates less that 0.2, 0.3, 0.5, and 1.0 mm/hour, and for rain rate larger than 10 mm/hour.

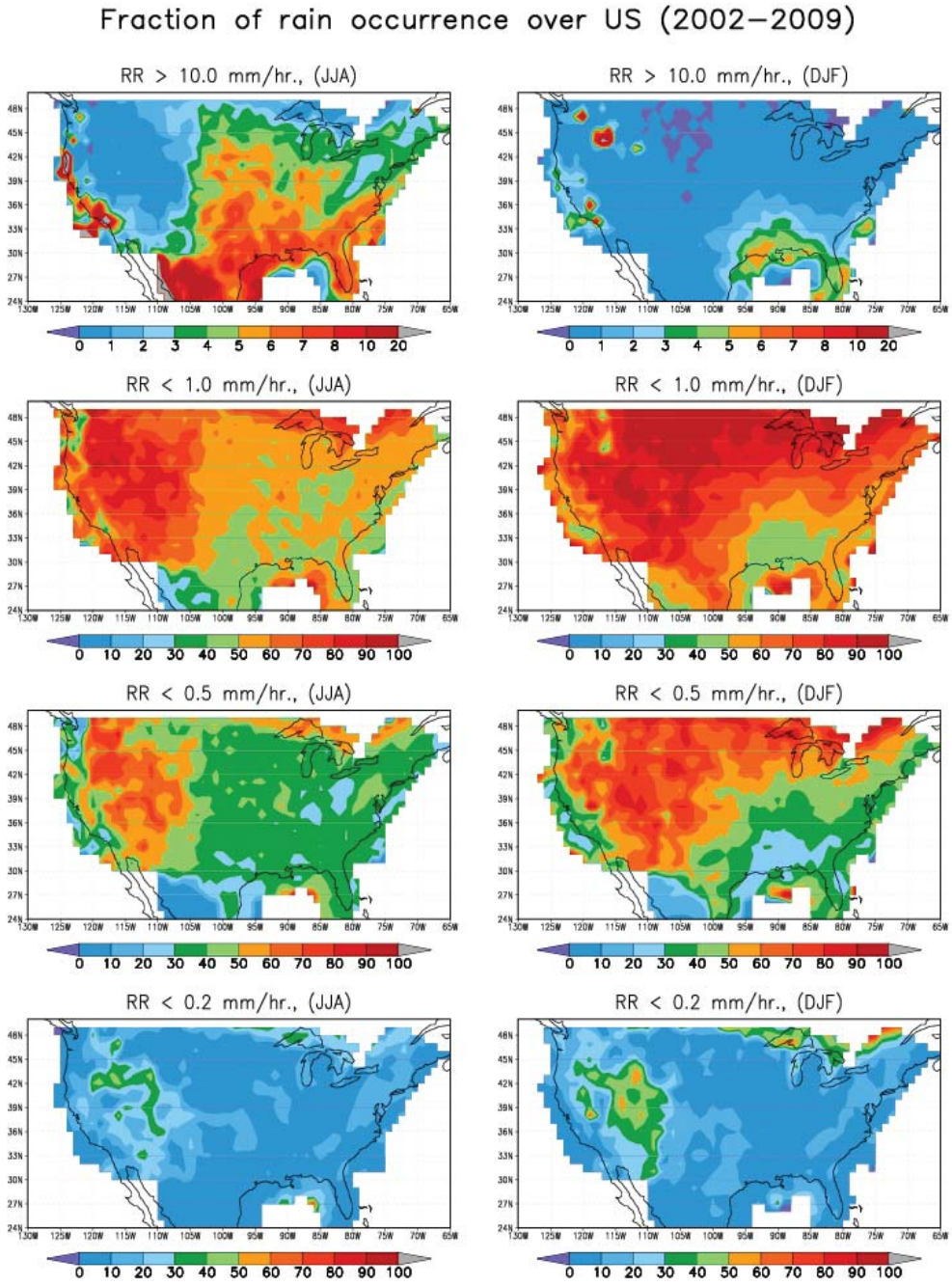

Figure 6a: Horizontal distributions of fraction of rain occurrence during the summer (JJA) and the winter (DJF) for rain intensity thresholds below 0.2, 0.5, 1.0 mm/hr., and above 10 mm/hr.

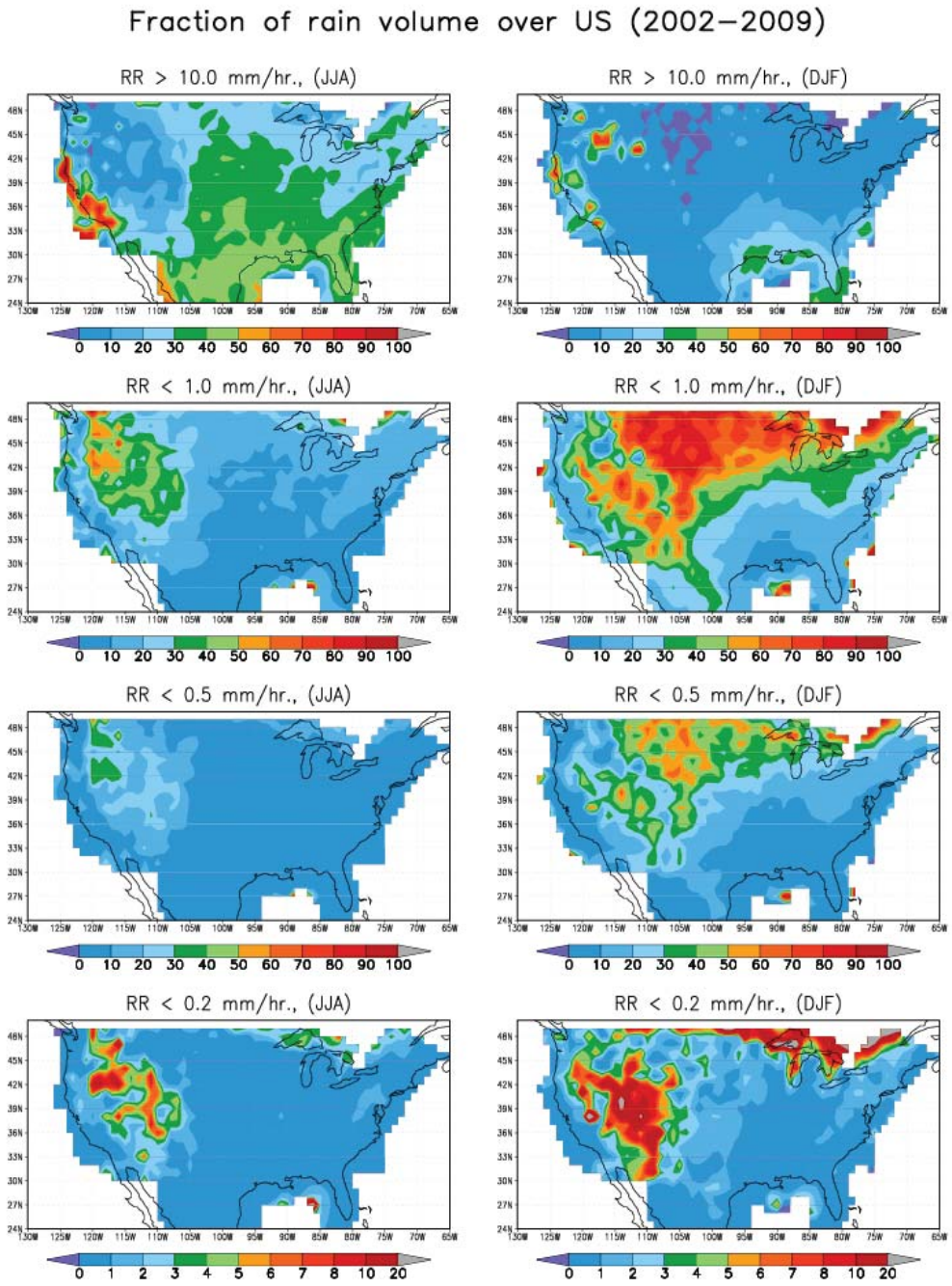

Figure 6b: Horizontal distributions of fraction of rain volume during the summer (JJA) and the winter (DJF) for rain intensity thresholds below 0.2, 0.5, 1.0 mm/hr., and above 10 mm/hr.

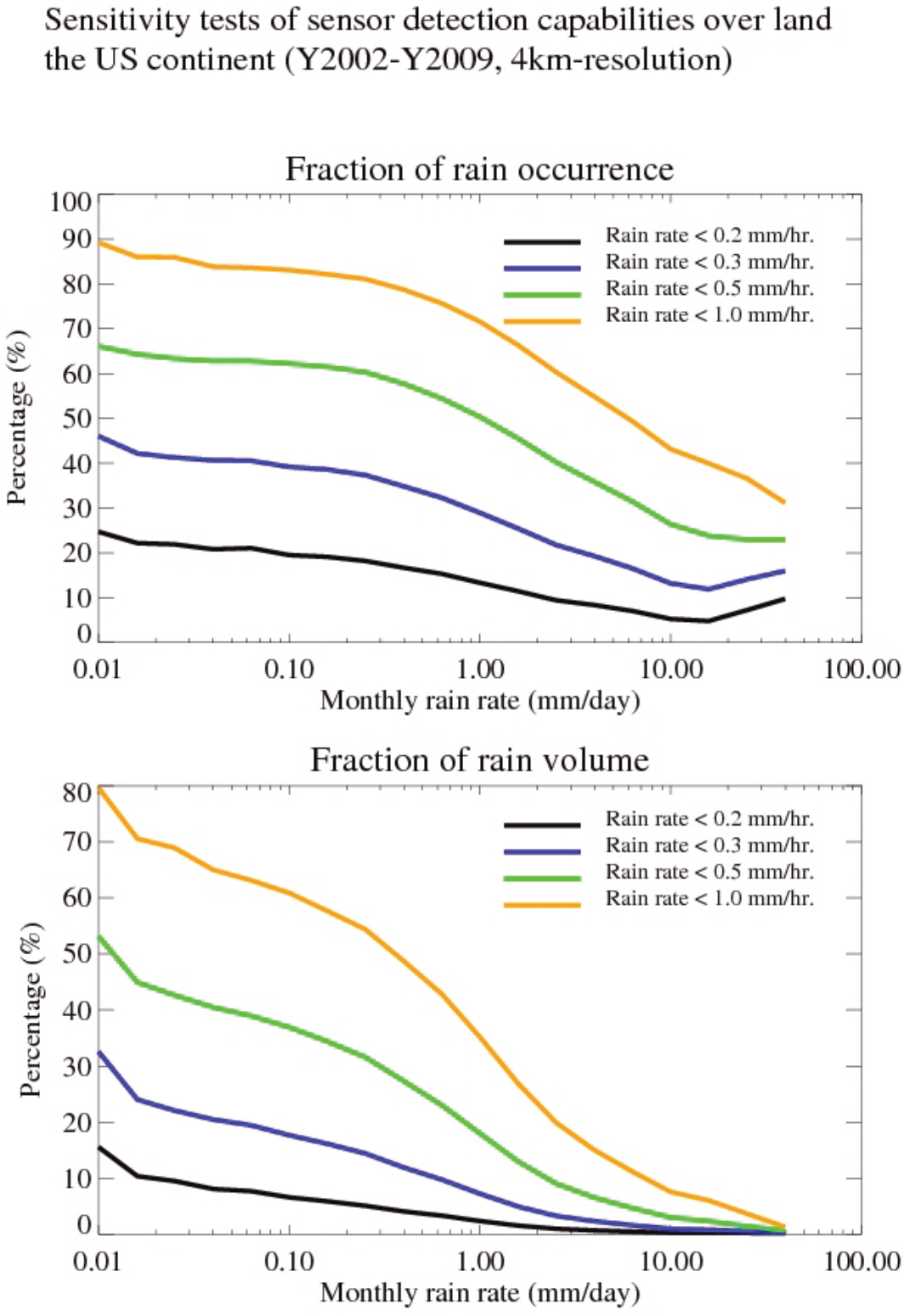

Figure 7: Fractions of rain occurrence (%) and rain volume (%) as functions of monthly mean rain rate derived on a 1°x1° grid.

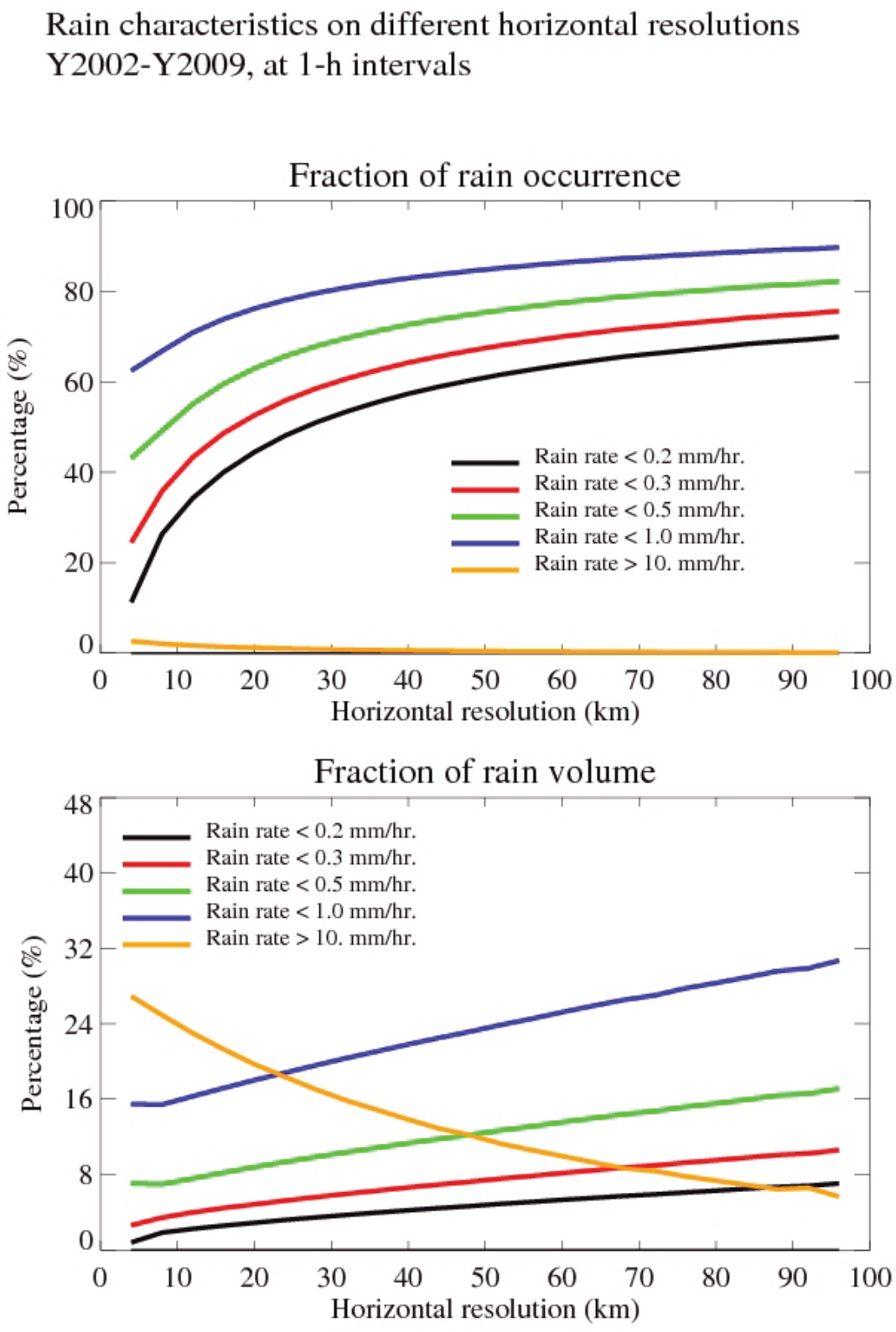

Figure 8: Variations of fractions of rain occurrence and rain volume as a function of horizontal resolutions for rain intensity thresholds larger than 10 mm/hr., and smaller than 0.2, 0.3, 0.5, and 1.0 mm/hr.

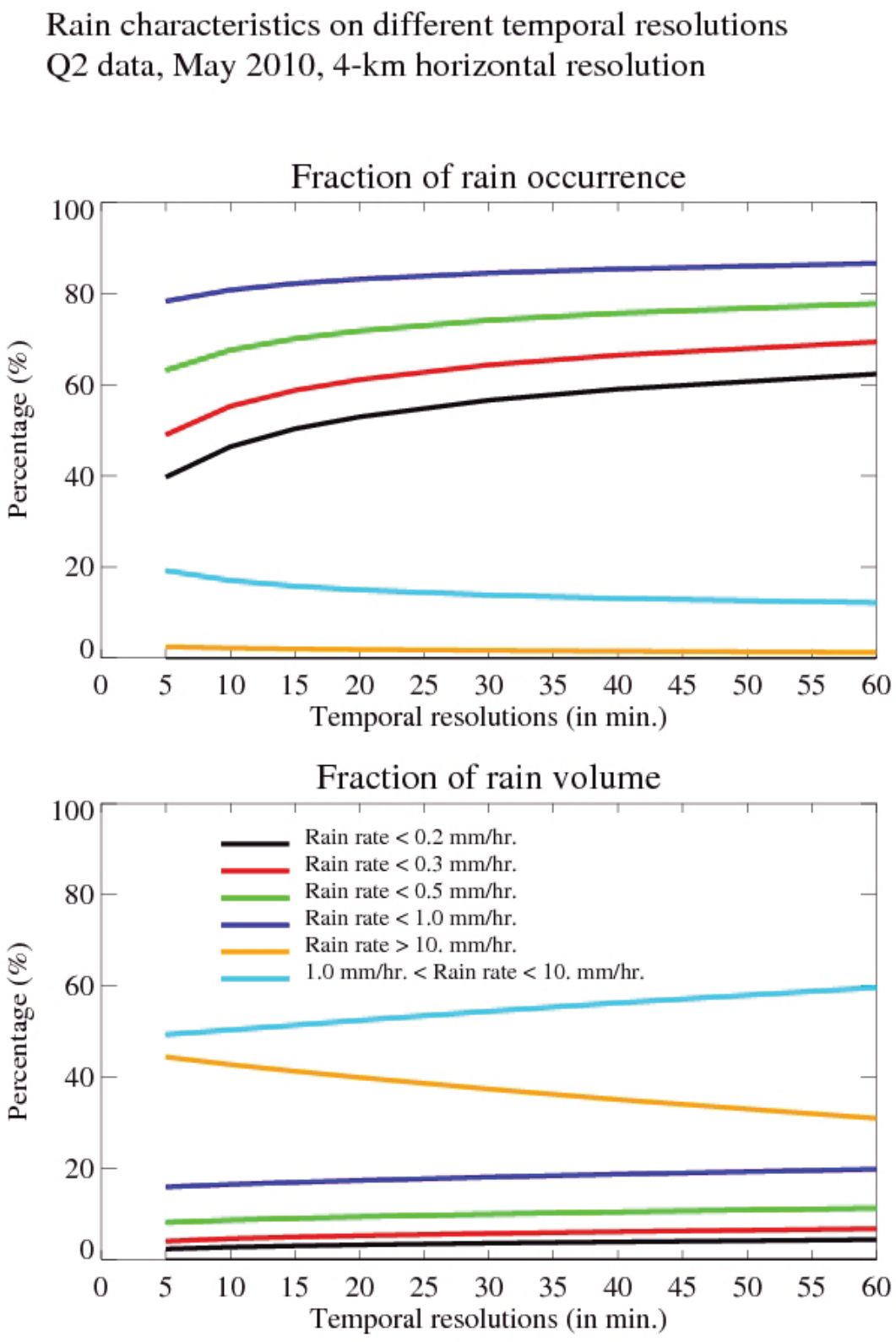

Figure 9: Variations of fractions of rain occurrence and rain volume as a function of temporal resolutions for rain intensity thresholds larger than 10 mm/hr., and smaller than 0.2, 0.3, 0.5, and 1.0 mm/hr.